Self-Alignment Capillary Gripper for Microfiber Manipulation

Longgang Song, Bo Chang, Yuhang Feng, Jialong Jin, and Quan Zhou, *Member, IEEE*

***Abstract*—The assembly and arrangement of microfibers have wide applications in biomedicine, material science, and microsystem. However, current micromanipulation methods for positioning and orientating individual microfibers are complex and hard to use. In this article, we report a novel self-alignment capillary gripper for microfiber manipulation that is facile and convenient. We determine the key parameters of the gripper including the required meniscus volume and the tip aspect ratio of the gripper through both numerical simulation and experimental investigation. A two-stage self-alignment process is employed to achieve high precision. The gripper can pick up and self-align microfibers with an aspect ratio of up to 300:1 at an accuracy of 2.1 ± 2.0 μm and $0.6 \pm 0.6°$ or better and create highly parallel linear arrays. The gripper is also versatile, where multiple types of microfibers including glass fibers, carbon fibers, dandelion seed fibers, and cat hairs can be picked up and self-aligned. Additionally, the gripper can construct two-dimensional patterns and plug a fiber into a microglass capillary.**

***Index Terms*—Capillary gripper, microfiber, micromanipulation, self-alignment.**

I. Introduction

FIBER assembly and arrangement is a crucial enabling technology with a multitude of applications in biomedicine, material science, and microsystems. Brain-machine interfaces [1], fiber-reinforced materials [2], and fiber sensors [3] are a few examples. Numerous methods for fiber assembly and arrangement have been developed, including electrospinning [4], 3-D printing [5], and field-assisted alignment employing electric [6] and magnetic fields [7], among others. These techniques can guide the orientation of fibers to a certain extent and arrange fiber into simple ordered structures such as threads, arrays, or interlaced matrices. However, the capability to control the position and orientation of individual fibers in the structure is limited.

Numerous techniques for controlling the position and orientation of individual fibers have been proposed, achieved through tedious manipulation with manual forceps [8] or automatic microrobotic tools [9] or fabrication with specially built high-precision alignment templates [10], [11]. Patel et al. [8] constructed a 16-channel, high-density carbon fiber electrode array by placing 16 carbon fibers on the conductive silver epoxy substrate with manual forceps. Chen et al. [9] used a multiaxis microrobot tool to place paper fibers parallelly on a V groove of a carbon pad with a spacing of 1 mm. Gillis et al. [10] used a 3D-printed alignment template to align fibers in microelectrode arrays for neural signal acquisition. Schwerdt et al. [11] fabricated fiber electrode arrays by aligning multiple carbon fibers using a glass micro-groove array mold. Even though these techniques can achieve the desired position and orientation of individual fibers, the level of complexity in manipulation, systems, or preparation steps restricts their usability and efficiency.

Capillary gripping is a versatile technique using a liquid meniscus for soft manipulation of microscale objects of various geometric shapes [12], [13], [14], including chips, spheres, cubes, cones, and a semicylinder. Recent research from the authors has shown that a capillary gripper can pick up and place single microfibers [15], [16], where the microfibers can be arranged in the groove of substrates. This approach allows for precise control over the spacing and direction of multiple individual microfibers. However, a patterned template was still required on the substrate, limiting the applicability of this technique. The authors have also previously demonstrated a self-alignment capillary gripper for microchips, with a 1:1 chip aspect ratio [17]. In addition, we have shown that a hydrophilic groove on a hydrophobic substrate can align a fiber by regulating the amount of liquid within the groove [18]. Those works prompted us the idea of a self-alignment capillary gripper. However, it remains a question if a capillary gripper can self-align objects with such a high aspect ratio as microfibers. This is especially the case considering that typical microfibers have a very small diameter, e.g., 10 μm, yet with a length in millimeters, leading to an aspect ratio of over two orders of magnitude.

In this article, we propose a facile self-alignment capillary gripper that utilizes a bar-shaped meniscus to pick up, self-align, and arrange microfibers of aspect ratio up to 500:1. The

Manuscript received 6 January 2023; revised 26 March 2023; accepted 1 May 2023. Date of publication 7 June 2023; date of current version 16 August 2023. Recommended by Technical Editor C. Clevy and Senior Editor Q. Zou. This work was supported by the National Natural Science Foundation of China under Grant 61703255. *(Corresponding authors: Bo Chang; Quan Zhou.)*

Longgang Song, Bo Chang, Yuhang Feng, and Jialong Jin are with the School of Mechanical and Electrical Engineering, Shaanxi University of Science and Technology, Xi'an 710021, China (e-mail: bs1805001@sust.edu.cn; changbo@sust.edu.cn; 1905003@sust.edu.cn; 1905004@sust.edu.cn).

Quan Zhou is with the Department of Electrical Engineering and Automation, School of Electrical Engineering, Aalto University, 02150 Espoo, Finland (e-mail: quan.zhou@aalto.fi).

This article has supplementary material provided by the authors and color versions of one or more figures available at https://doi.org/10.1109/TMECH.2023.3276064.

Digital Object Identifier 10.1109/TMECH.2023.3276064

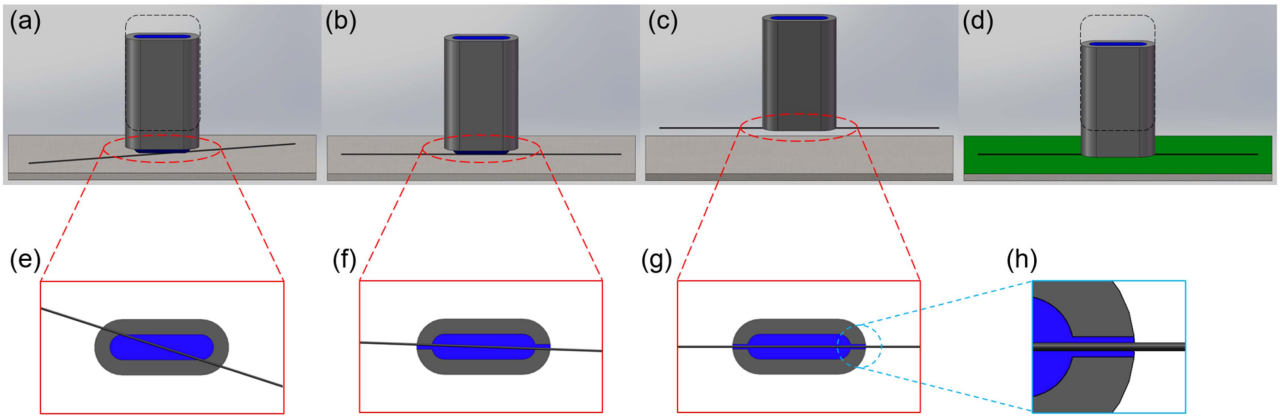

Fig. 1. Schematic of the manipulation procedure of the capillary self-alignment gripper: (a) Pick-up; (b), (c) two-stage self-alignment and transport; and (d) placement; (e)–(g) shows the position of the fiber at the end of the gripper tip; (h) view of one end of the gripper tip, where the fiber is aligned inside a groove.

self-alignment capillary gripper is also versatile and capable of handling fibers ranging from carbon fibers, glass fibers, to dandelion seed fibers, and cat hairs.

The rest of this article is organized as follows. Section II introduces the concept of the self-alignment capillary gripper and the apparatus used for experimental studies. Section III discusses the simulation analysis of the gripper and the design of the system parameters of the gripper, mainly the meniscus volume, the tip aspect ratio, the influence of friction on fiber self-alignment, and the high-precision alignment strategy. Section IV experimentally evaluates the performances of the gripper, including the maximum pick-up force, the capability of self-aligning multiple types of fiber, and the placement and patterning capabilities of the gripper. Finally, Section V concludes this article.

II. Concept and Apparatus

A. Working Principle and Alignment Strategy

The self-alignment capillary gripper utilizes the surface tension of a bar-shaped meniscus between the gripper tip and the microfiber, and the groove at the two ends of the gripper tip to realize fiber pick-up and self-alignment. Where the surface tension provides both the fiber pick-up force and fiber restoring force, the groove is used to further refine and fix the fiber alignment position. Fig. 1(a)–(d) illustrates the manipulation procedure of the gripper during the pick-up, self-alignment, transport, and placement of fibers. First, a gripper with a bar-shaped meniscus [the blue area in Fig. 1(e)] moves downward, then the meniscus contacts and wets the fiber and forms a meniscus bridge with the fiber [see Fig. 1(a)]; next, the liquid surface tension picks up and self-aligns the fiber to the long axis of the meniscus [see Fig. 1(b) and (f)]; after picking up, the gripper moves upward while the meniscus at the gripper tip is reduced by a syringe pump, consequently the fiber is fixed in the groove [see Fig. 1(c) and (g)]; finally, the gripper transports the fiber onto the substrate [see Fig. 1(d)]. Fig. 1(h) shows that a view of one end of the gripper tip, where the fiber is aligned inside a groove.

In this article, we focus on the manipulation of typical microfibers with a diameter of around 10 μm and lengths of a couple of millimeters. However, fibers with diameters up to 24 μm have also been tested in the experimental study.

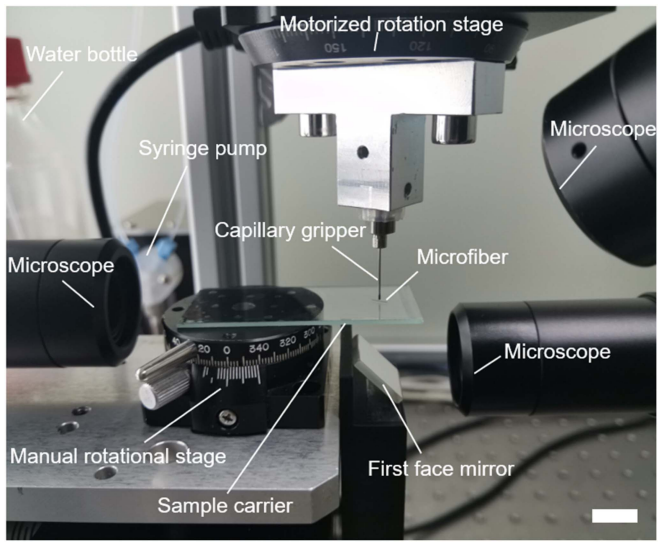

Fig. 2. Robotic platform for the experimental study. Scale bar: 10 mm.

B. Experimental Platform

We have constructed a miniaturized robotic system to study the proposed capillary gripper and its application, as shown in Fig. 2. The robotic system consists of a motion system, a liquid dispensing system, and a vision system. The motion system consists of three motorized linear stages (one M-414.2PD and two M-111.1DG by Physik Instrumente, Karlsruhe, Germany), one motorized rotation stage (ERSP60 by Sanying Motion Control Instruments Ltd., Tianjin, China), and one manual rotation stage (RSP40-L by Weixianfeng, Guangdong, China). The three linear stages are used to position the sample carrier in three dimensions with a precision of 0.5 μm. The rotation stage is used to rotate the gripper and the sample carrier, respectively. The positioning of the sample carrier and the gripper are

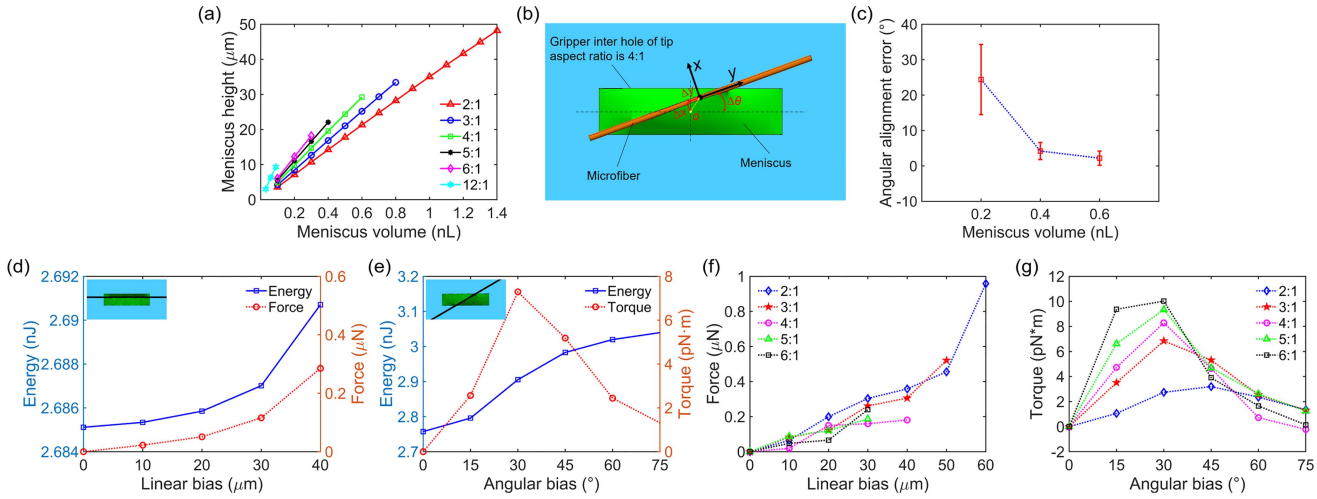

Fig. 3. (a) Relationship between the meniscus volume and the meniscus height obtained using numerical software Hydro. (b) Schematic diagram of the linear bias, the angular bias, and the grasping bias. (c) Experimental results of the influence of meniscus volume on angular alignment error for the 4:1 gripper tip. Numerically calculated surface energy, force and torque at different linear and angular biases: (d) surface energy of the water meniscus and restoring force versus the linear bias for the 4:1 gripper tip, the inset shows a Surface Evolver model of a linear bias is 20 μm; (e) surface energy and restoring torque versus angular bias for the 4:1 gripper tip, the inset shows a Surface Evolver model of an angular bias is 30°; (f) restoring force versus linear bias for different tip aspect ratios; (g) restoring torque versus angular bias for different tip aspect ratios.

controlled by a custom-built automation program. The liquid dispensing system can dispense a precise meniscus volume at the gripper tip using a precision syringe pump (Tecan Group Ltd., Männedof, Switzerland). The syringe pump is also used to reduce the meniscus volume, typically 0.6 nl, from the gripper tip. The vision system consists of three microscopes with CCD cameras (Point Grey BFLY-U3-23S6C-C by Edmund Optics, USA) to observe the meniscus volume at the gripper tip, the fiber self-alignment process, and the motion of the fiber. The microfiber self-alignment process is observed from the bottom in a reflected image through a first surface mirror mounted on the stage at a 45° angle.

III. Design of the Gripper

Several parameters affect the performance of the self-alignment capillary gripper, including the size, the tip aspect ratio, the meniscus volume, and the initial position bias in relation to the fiber. If we employ the concept of shape matching widely used in capillary self-alignment [19], [20] the gripper should be similar in size to the fiber. Due to the great aspect ratio and small diameters of the fiber, controlling such a long bar-shaped meniscus will be delicate. In addition, matching the two orders of magnitude in aspect ratio will make the gripper unnecessarily large, which in turn will greatly reduce the selectivity of the gripper during manipulation. Therefore, we employ a two-stage self-alignment strategy, first, a bar-shaped meniscus roughly aligns the fiber, then the grooves at both ends of the gripper tip further align and fix the fiber in location [see Fig. 1(f) and (g)]. This allows us to construct a gripper using readily available components such as a commercial stainless needle to prepare self-alignment capillary grippers.

A. Tip Aspect Ratio

The tip aspect ratio, the ratio between the long axis and the short axis of the inner hole of the tip, is likely the most important dimensional parameter of the gripper, which greatly affects the energy gradient and restoring force of the first self-alignment process. A tip aspect ratio of 1:1 on a round tip will lead to no alignment. Intuitively, the higher the ratio, the better the self-alignment. However, the matter is more complicated when we consider issues such as the confinable volume of the liquid meniscus on the tip, the height of the liquid meniscus that facilitates manipulation, and the interaction between the fiber, meniscus, and the bottom surface of the gripper.

In this article, we focus on the design of tips fabricated using readily available commercial stainless needles (with an outer diameter of 500 μm and an inner diameter of 280 μm, more details see Appendix A). We studied grippers with different tip aspect ratios varying from 2:1 to 12:1 [see Table I in Appendix A for the actual parameters and Fig. 9(a) for the images of the tips]. There are two ways to confine a meniscus at the tip of the gripper, either using the inner edge (the inner hole) or the outer edge. We confine the liquid meniscus using the inner edge of the gripper since the confinement of the meniscus is more reliable. We used a glass fiber of 4 mm × ∅ 13 μm, a widely used fiber and the main subject of study in this article, as the specimen in both experimental and simulation studies.

First, we calculated the relationship between the meniscus volume and the meniscus height for different tip aspect ratios using HyDro [21] [see Fig. 3(a)]. Accordingly, we can also obtain the maximum confined meniscus volume of the gripper tips. For the grippers with tip aspect ratios of 2:1, 3:1, 4:1, 5:1, 6:1, and 12:1, the respective maximum confined meniscus volume is 1.4 nL, 0.8 nL, 0.6 nL, 0.4 nL, 0.3 nL, and 0.09 nL. We experimentally studied the influences of meniscus volume

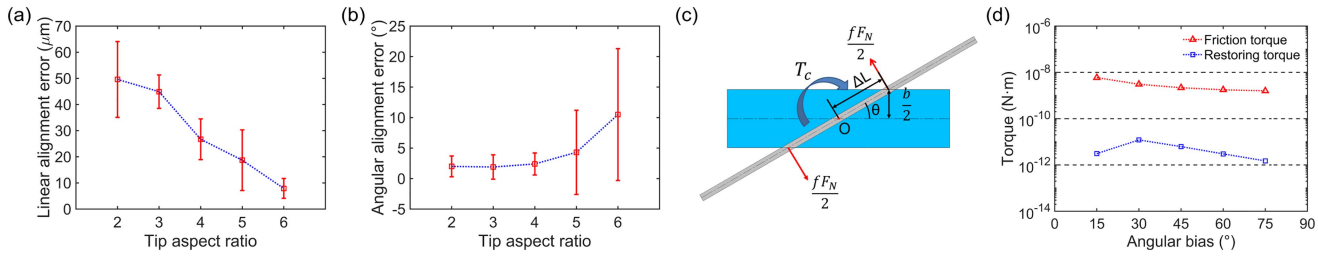

Fig. 4. Experimental results of (a) the influence of tip aspect ratio on linear alignment error, and (b) the influence of tip aspect ratio on angular alignment error; (c) schematic diagram of the restoring torque T_c and the friction torque T_f; (d) the estimated magnitude of restoring torque T_c and friction torque T_f.

on self-alignment using a gripper with a tip aspect ratio of 4:1 and the glass fiber. Three meniscus volumes of 0.2 nL, 0.4 nL, and 0.6 nL (the maximum confinable volume) are used in this article. The initial linear bias, angular bias, and grasping bias between the fiber and the gripper were 0 μm, 30°, and 0 μm, respectively. The linear bias refers to the distance between the projection of the fiber at the gripper bottom and the center of the gripper tip ["o" in Fig. 3(b)], labeled as Δx. The angular bias is the angle between the projection of the fiber at the gripper bottom and the long axis of the gripper tip, labeled as $\Delta\theta$. The grasping bias refers to the distance between the center of the mass of the fiber and the center of the gripper along the axis of the fiber, labeled as Δy [see Fig. 3(b)]. The experimental results show that the angular alignment errors are $24.4 \pm 9.9°$, $4.2 \pm 2.4°$, and $2.2 \pm 2.0°$, for meniscus volume of 0.2 nL, 0.4 nL, and 0.6 nL, respectively, where each experiment was repeated five times [see Fig. 3(c)]. We attribute the large errors to dry contacts between the fiber and the gripper tip surface, which hinders the self-alignment, where a smaller meniscus volume leads to a greater chance of failure. Therefore, the maximum confinable meniscus volume for the gripper tips was used in all the following experiments.

The tip aspect ratio will also impact the restoring force and torque. The restoring force and torque for different tip aspect ratios can be estimated using Surface Evolver [22]. The restoring force is the gradient of the surface energy

$$\overrightarrow{F_c}(\Delta x) = -\nabla E(\Delta x) \tag{1}$$

where E is the surface energy of the liquid meniscus, and Δx is the linear bias. Accordingly, the restoring torque can also be obtained

$$\overrightarrow{T_c}(\Delta\theta) = -\nabla E(\Delta\theta) \tag{2}$$

where $\Delta\theta$ is the angular bias.

We simulated the restoring forces and torques at the different linear and angular biases for the glass fiber on the stainless gripper tip [see Fig. 3(d)–(g)], where the Surface Evolver code can be found at [23]. The glass fiber used in the simulation has a diameter of 13 μm and a contact angle of 15°, the water surface tension is $\gamma = 72.8$ mN/m and the water contact angle of the gripper surface is 62°. Fig. 3(d) and (e) shows the energy, restoring force, and restoring toque for the tip with a tip aspect ratio of 4:1. As expected, the surface energy and the restoring force increase with the increase of the linear bias, and the meniscus reaches equilibrium when the linear bias is zero [see Fig. 3(d)]. Fig. 3(e) shows that the energy also increases with the increase of the angular bias. However, the restoring torque has a maximum of around 30°. Fig. 3(f) shows the relationship between linear bias and restoring force for tips with different tip aspect ratios, where the restoring force increases with the increase of linear bias for all tip aspect ratios. The difference in the maximum linear bias in the curves is the result of the difference in the size of the meniscus for tips of different aspect ratios (see Table I in Appendix A). Fig. 3(g) shows the relationship between angular bias and restoring torque for different tip aspect ratios. The restoring torque follows a similar trend except for the tip aspect ratio 2:1 where the maximum peak occurs at 45°. The results show that a high tip aspect ratio may lead to a stronger restoring torque at an angular bias of 30° or below, but the advantage is not clear beyond 30°.

We also experimentally studied the effect of different tip aspect ratios on the fiber self-alignment when the initial linear bias is 0 μm and the angular bias is 30° with ten repetitions [see Fig. 4(a) and (b)]. The experimental results show that the linear alignment error decreases with the increase in tip aspect ratio [see Fig. 4(a)]. For angular alignment error, the results are similar for tip aspect ratio less than or equal to 4:1 [see Fig. 4(b)], $2.0 \pm 1.7°, 1.9 \pm 2.0°, 2.4 \pm 1.8°$ for tip aspect ratio of 2:1 to 4:1. However, the angular alignment error increases rapidly for the tip aspect ratio of 5:1 and 6:1, $4.3 \pm 6.9°$, $10.5 \pm 10.8°$, respectively, which can be attributed to the decrease of the maximum confinable meniscus volume of 0.4 nL and 0.3 nL, versus 1.4 nL, 0.8 nL, 0.6 nL for the cases of 2:1 to 4:1.

Furthermore, we experimentally studied a gripper with a tip aspect ratio of 12:1. Even though the width of the inner hole (35 μm) of the gripper matched best the fiber diameter (13 μm), self-alignment does not occur in all experiments. We attribute the failure to low meniscus height (9 μm) at the maximum confinable volume, which caused dry contact between the fiber and the gripper surface.

In the following experiments, we use the gripper with a tip aspect ratio of 4:1 since it has a good compromise between linear alignment error and angular alignment error.

B. Influence of Friction on Fiber Self-Alignment

To understand the effect of dry friction during fiber self-alignment, we numerically calculated the restoring torque T_c

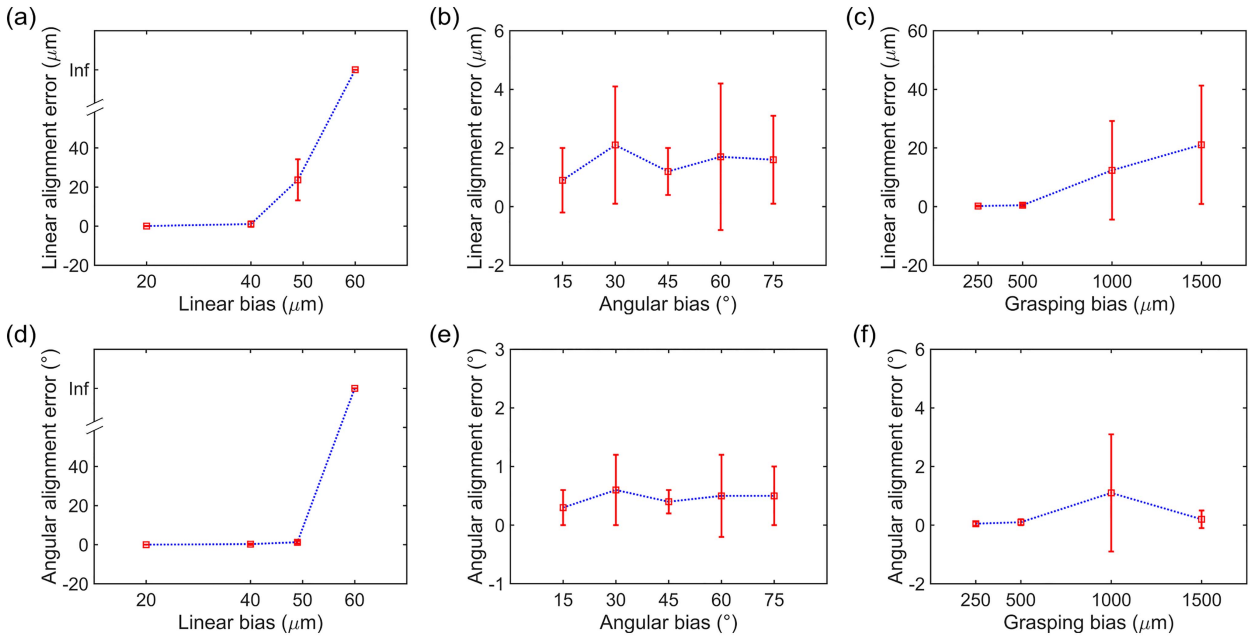

Fig. 5. Experimental results of the effect of the linear bias, the angular bias, and the grasping bias on self-alignment error. (a) Effect of linear bias on linear alignment error. (b) Effect of angular bias on linear alignment error. (c) Effect of the grasping bias on linear alignment error. (d) Effect of the linear bias on angular alignment error. (e) Effect of angular bias on angular alignment error. (f) Effect of the grasping bias on angular alignment error.

and the friction torque T_f for the tip aspect ratio of 4:1 and the meniscus volume of 0.2 nL [see Fig. 3(c)]. The schematic diagram of the capillary restoring torque T_c and the frictional torque T_f is shown in Fig. 4(c). The frictional torque T_f is estimated by

$$T_f = fF_N\Delta L \tag{3}$$

where f is the friction coefficient between the fiber and the surface of the gripper tip $f = 0.6$. F_N is the normal force $F_N = F_C - mg = F_C - \rho Vg$. F_C is the capillary force in the vertical direction pulling the fiber toward the gripper tip surface, estimated by Surface Evolver. Glass fiber is used in the simulation, with density $\rho = 2500\ \mathrm{kg/m^3}$ and volume $V = 2\pi rL$, $r = 6.5\ \mu$m, $L = 4$ mm, and $g = 9.8\ \mathrm{m/s^2}$. Here, the ΔL is the distance between the point of action to the point O, which can be calculated by

$$\Delta L = \frac{b}{2\sin\theta} \tag{4}$$

where $b = 98\ \mu$m is the inner hole width of the gripper tip, and θ is the angular bias. The magnitudes of the restoring torque and the friction torque are shown in Fig. 4(d). The results show that the friction torque is much larger than the restoring torque (about two orders of magnitude) when the fiber and the gripper have dry contact. Therefore, once the fiber contacts the gripper, the friction torque will hinder the self-alignment of the fiber, leading to self-alignment failures.

C. High-Precision Alignment

To achieve a higher precision alignment than reported in Section III-A, we fabricated grooves at the two ends of the long axis of the 4:1 gripper tip [see Fig. 9(b) and (c) in Appendix B for details and the fabrication procedures]. The grooves have a width of 27 μm and a depth of 15 μm. When a fiber contacts the meniscus of the gripper, the bar-shaped meniscus self-aligns the fiber roughly to the long axis of the gripper. Then, the grooves further align and fix the fiber in location when the meniscus is reduced.

We experimentally studied the influence of the linear bias, angular bias, and grasping bias on the self-alignment using a gripper of 4:1 tip aspect ratio with grooves and glass fiber of 4 mm $\times$ $\varnothing$13 μm, where each experiment was repeated five times. Fig. 5 shows the experimental results. Four linear biases 20 μm, 40 μm, 49 μm, and 60 μm are used in the study when angular bias is 0° and grasping bias is 0 μm. Fig. 5(a) and (d) shows the effect of linear bias on linear and angular alignment errors. The results show that the fiber self-aligned well when the linear bias is 20 μm and 40 μm, with linear alignment errors of 0.1 ± 0.1 μm and 1.1 ± 1.4 μm and angular alignment errors of $0.1 \pm 0.1°$ and $0.3 \pm 0.4°$, respectively. When the linear bias is 49 μm, the half-width of the inner hole of the gripper tip, the linear alignment error is 23.7 ± 10.5 μm, and the angular alignment error is $1.3 \pm 0.6°$. We attributed the large error to the unreliable contact of the meniscus and the microfiber. When the linear bias is 60 μm, the fiber did not self-align [the alignment error is expressed as Inf in Fig. 5(a) and (d)]. We attributed this to the meniscus failing to contact the fiber since half of the width of the inner hole is 49 μm, less than the linear bias. Fig. 5(b) and (e) shows the experimental results of the influence of angular bias on the linear and angular alignment errors when the linear and grasping biases are 0 μm. The results show that the maximum linear alignment error is 2.1 ± 2.0 μm at 30° bias and the respective angular alignment error is $0.6 \pm 0.6°$. Fig. 5(c) and (f) shows the effect of the grasping bias on linear

and angular alignment errors when the linear and angular biases are not present. The results show that the grasping bias of 250 μm and 500 μm have no observable impact on alignment error (linear alignment errors are 0.2 ± 0.2 μm and 0.5 ± 0.4 μm, and angular alignment errors are $0.1 \pm 0.1^\circ$ for both cases). With the increase of grasping bias, the angular alignment error does not change significantly, but the linear alignment error increases significantly. When the grasping bias is 1000 μm and 1500 μm, the linear alignment errors are 12.4 ± 16.8 μm and 21.1 ± 20.2 μm, and the angular alignment errors are $1.1 \pm 2.0^\circ$ and $0.2 \pm 0.3^\circ$, respectively.

We also experimentally studied the combined effect of multiple types of biases on self-alignment, which shows that the self-aligning capillary gripper has good bias tolerance. For the linear bias of 20 μm, the angular bias of 30°, and the grasping bias of 250 μm, we achieved a linear alignment error of 0.7 ± 0.2 μm, and angular alignment error of $0.2 \pm 0.1^\circ$. For the linear bias of 40 μm, the angular bias of 30°, and the grasping bias of 500 μm, we achieved a linear alignment error of 1.6 ± 0.5 μm, and angular alignment error of $0.5 \pm 0.1^\circ$.

Noticeably, the self-alignment process is generally fast, where each self-alignment step takes around a hundred milliseconds, while the two-stage self-alignment process could take around four seconds, where most of the time is used to lift the gripper from the substrate (see the Supplementary Movie). We also conducted stability tests for the gripper during accelerated motion. The gripper, with the aligned fiber, was moved linearly at 100 mm/s as well as rotated at 30°/s. In both experiments, the fiber remained stable at the tip of the gripper in repetitive tests.

IV. Gripping Performance and Arrangement

A. Maximum Pick-Up Force

When the gripper picks up the microfiber, the fiber is subjected to three forces, the pick-up force F_1 from the liquid meniscus, the gravitational force G, and the adhesion force F_2 between the fiber and the substrate. Fig. 6(a) shows a schematic diagram of the force on the fiber when the gripper picks up the fiber. The necessary conditions for the gripper to pick up the fiber successfully is

$$F_1 > G + F_2 \tag{5}$$

The maximum pick-up force is an important measure to evaluate the pick-up ability of the gripper. We have experimentally obtained the maximum pick-up force using a carbon fiber, which was restricted from vertical movement by two metal rings [see Fig. 6(b)]. In the experiments, the gripper first touched the carbon fiber with the meniscus, then moved up slowly, bending the carbon fiber until the meniscus ruptured [Fig. 6(b) shows the moment before the rupture]. Using a gripper with a tip aspect ratio of 4:1 and an initial meniscus volume of 0.6 nL, we measured the maximum deformation of the carbon fiber before the rupture to calculate the maximum pick-up force. By considering the carbon fiber as a rigid beam, we employed a classical simply supported beam model to estimate the maximum pick-up force that the gripper can exert. The maximum pick-up force was calculated by

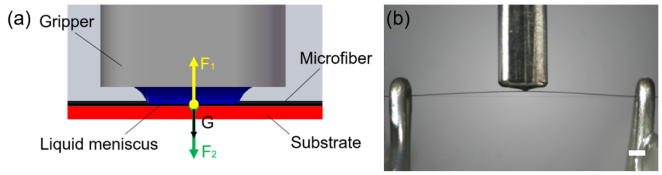

Fig. 6. (a) Schematic diagram of the forces acting on the fiber. (b) Deformation of the fiber at the moment before it was separated from the gripper. Scale bar: 200 μm.

$$F = -\frac{48EIW}{L^3} \tag{6}$$

where W is the maximum deflection of the carbon fiber before the meniscus breaks, E is the elastic modulus (210 GPa for the carbon fiber), the moment of inertia $I = \pi d^4/64$, the length of the supported beam $L = 3$ mm, the carbon fiber diameter $d = 8$ μm. In this experiment, we recorded $W = 56.6 \pm 8.3$ μm. Therefore, the respective maximum pick-up force $F = 4.2 \pm 0.6$ μN.

The gravitational force on a glass fiber of 4 mm × ∅ 13 μm with a density of 2500 kg/m^3 is $G = 1.3 \times 10^{-2}$ μN. So the weight of glass fiber is two orders of magnitude smaller than the maximum pick-up force and can be ignored. The adhesion force F_2 between the glass fiber and the substrate may have different contributions, including van der Waals force, electrostatic force, and capillary force. We used a superhydrophobic substrate to avoid the influence of capillary force. In addition, both the capillary gripper and the motion platform are grounded, so the electrostatic force is insignificant. The adhesion force F_2 is then mainly contributed by the van der Waals force. Using the classical cylinder and plane model, we can estimate the van der Waals force [24]

$$F_{\text{vdW}} = \frac{-A\sqrt{R}L}{8\sqrt{2}D^{5/2}} \tag{7}$$

where A is the Hamaker Constant, R is the fiber radius, L is the fiber length, and D is the distance between the fiber and the substrate. The Hamaker Constant A between the glass fiber and the substrate is in the order of 10^{-19} J [24]. The roughness of the substrate and the linearity of the fiber determines the distance D. Take D the mean roughness of the Glaco substrate of $10^{-2}\mu m$ [25] and a perfectly straight fiber, the F_{vdW} should be in micronewtons, which is at the same level as the maximum pick-up force. However, the fiber is not perfectly straight, making the effective distance between the fiber and the substrate much greater than the value of the surface roughness, hence the combined contribution of the gravitational force and the adhesion force will be much less than the maximum pick-up force.

B. Manipulation of Other Artificial and Natural Fiber-Like Materials

We experimentally tested the self-alignment of both artificial fibers and natural fibers, including carbon fibers, glass fibers, dandelion seed fibers, and cat hair. The fiber diameter ranges from 8 μm to 24 μm, and the length is 4 mm. Fig. 7 shows

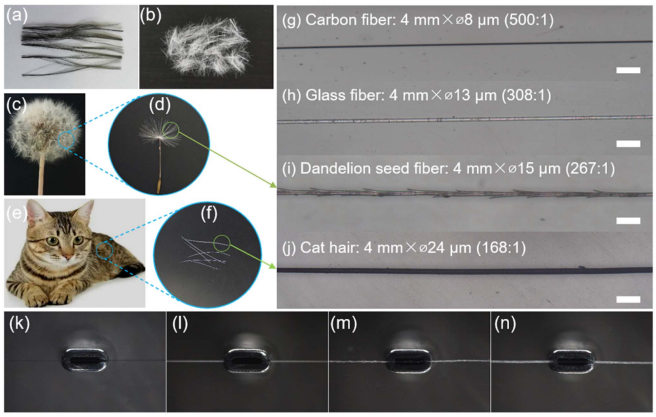

Fig. 7. Demonstration of capillary self-alignment of different types of microfibers on the gripper: (a) Carbon fibers; (b) glass fibers; (c), (d) dandelion seed fibers; (e), (f) cat hairs. (g)–(j) Optical photos of single fiber and the respective fiber diameter: (g) Carbon fiber; (h) glass fiber; (i) dandelion seed fiber; (j) cat hair. (k)–(n) Optical picture of the self-alignment result between the capillary gripper and (k) a carbon fiber; (l) a glass fiber; (m) a dandelion seed fiber; (n) a cat hair. Scale bar: 100 μm.

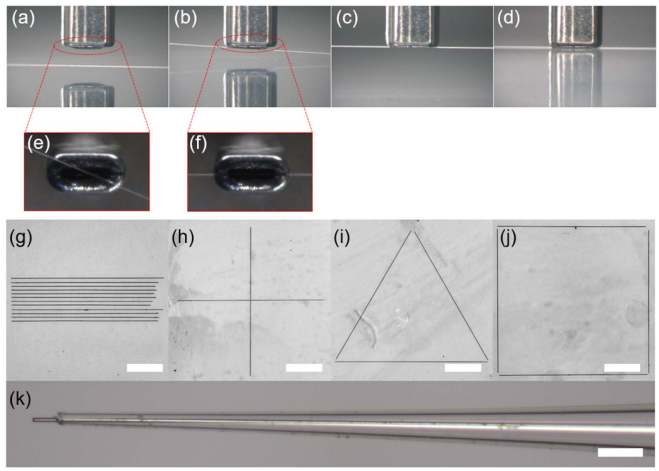

Fig. 8. Placement demonstration of the capillary self-alignment gripper. (a)–(f) Fiber manipulation procedure. (g)–(j) Results of two-dimensional fiber patterning. Scale bar: 1 mm. (k) A carbon fiber inserted into a glass capillary with 16 μm inner diameter. Scale bar: 100 μm.

the optical micrographs of different types of microfibers and the self-alignment results of the microfiber on the gripper. All fibers were initially placed on the superhydrophobic substrate (see Appendix C) randomly, and then self-align with the gripper after being picked up. It is worth noting that although the dandelion seeds fiber is curved and has tiny spikes, the gripper can still pick up and self-align the fiber. Examples of the self-alignment experiments can be found in the Supplementary Movie.

C. Placement and Patterning

The 2-D distribution and the alignment of microfibers have a major effect on the mechanical, electrical, and thermal properties of fiber-reinforced materials. Here, we demonstrate the application in 2-D patterning using our self-alignment capillary gripper. We pick up and self-align randomly placed microfibers from the substrate, and then place the fibers at the target position on a polydimethylsiloxane (PDMS) substrate. To release the microfiber, we slightly push the gripper on the viscoelastic PDMS substrate for about 5 μm, where the strong adhesion properties of PDMS facilitate the easy release of the fiber. Fig. 8(a)–(f) shows the process and results of the pick-up, self-alignment, transport, and release of glass fiber using the 4:1 gripper tip. We also patterned glass fibers (length ~4 mm) into a densely packed linear array of 12 fibers with a spacing of 100 μm [see Fig. 8(g)]. The resultant array has a spacing error of 1.8 ± 10.3 μm and an angular error of $0.0 \pm 0.1^\circ$. It is interesting to note that the angular accuracy after placement is greater than the results on the gripper tip [see Fig. 5(e)], we attribute this to the additional mechanical self-alignment of the fiber to the grooves during placement due to slightly pushing the gripper tip into the PDMS surface. On the other hand, while the mean spacing error of 1.8 μm may be attributed to the linear alignment error of the fiber on the gripper, the uncertainty of 10.3 μm in spacing error may come from the interaction between the fiber and the viscoelastic surface during and after release. Additionally, we can also construct other patterns including a cross, a triangle, and a square [see Fig. 8(h)–(j)]. The process of constructing the cross structure can also be found in the Supplementary Movie. Inserting a microfiber into micropores is also an important task in industry and manufacturing. Fig. 8(k) shows that a carbon fiber with a diameter of 8 μm was inserted into a glass capillary with an inner diameter of 16 μm using the gripper, where the fiber was pushed inside the glass capillary using the side wall of the gripper tip after the initial insertion.

V. Conclusion

This article reported a novel self-alignment capillary gripper that is easy to fabricate using commercially available off-the-shelf components. The gripper employed a two-stage self-alignment process that can manipulate a wide range of microfibers. We noticed that the height of the meniscus has a major impact on the performance of the gripper besides the tip aspect ratio. The performance of the gripper is also not very sensitive to the positioning of the gripper and the microfiber, where a linear bias of up to 40 μm, an angular bias of up to 75°, and a grasping bias of up to 500 μm has little impact on the self-alignment performance. The gripper also performs well with a modest combination of linear bias, angular bias, and grasping bias. The gripper has been tested for fibers with diameters from 8 μm up to 24 μm. For a much greater diameter, the current groove width of 27 μm will be insufficient, and the groove should be redesigned to be compatible with the diameter of the fiber. For a much smaller diameter, the restoring torque will be significantly smaller, which may be a problem if there is friction or strong viscous force. The capillary length should also be considered when determining the diameter of the fiber that can be manipulated.

In this article, we used a superhydrophobic surface for pick-up and PDMS substrate for placement to make the process highly robust, since the focus of the research is on the self-alignment gripper. Other surfaces, such as paper tissue, glass, silicon,

stainless steel, and copper can also be used as the surface for reliable placement [16]. Microfibers can also be picked up on those surfaces, even though the success rate is low when the contact angle is less than 50°, in the case of paper tissue, glass, and silicon [16], and a hydrophobic surface is generally preferred for pick-up. Nevertheless, the dynamics of the fiber during pick-up and placement on different surfaces deserve more thorough study.

Compared with the existing single fiber manipulation technique, the proposed self-alignment capillary gripper requires no template, and can pick up and align a fiber in seconds, compared to the reported manual approach and microrobotic approach, which usually takes minutes. The self-alignment capillary gripper also has great angular accuracy, achieving an alignment error of $0.6 \pm 0.6°$ on the gripper and $0.0 \pm 0.1°$ in the patterned linear array, compared with $5.1 \pm 3.1°$ and $1.4 \pm 0.8°$ for the reported manual approach and microrobotic approach [9]. With its performance, versatility, readily available components, and easy fabrication process, the gripper has great application potential.

APPENDIX

A. Fabrication of the Self-Alignment Capillary Gripper

The self-alignment capillary gripper was fabricated from a flat mouth stainless steel needle (25G by Zhenen Industrial Products Franchise Store, China) with an outer diameter of 500 μm and an inner diameter of 280 μm [see Fig. 9(a)]. The tip of the needle (length 1.5 mm) was pressed flat using a customized motorized precision fixture, which consists of a motorized linear stage (M-414.3PD by Physik Instrumente, Germany) and two stainless steel clamping blocks. The different tip aspect ratios of grippers are obtained by controlling the spacing of clamps. The bottom of the gripper was then ground with 3000 grit sandpaper on a rotating platform. Table I shows the inner hole dimensions of grippers with different tip aspect ratios.

TABLE I
INNER HOLE DIMENSIONS OF THE GRIPPER TIPS

Tip aspect ratio	Inner hole length (μm)	Inner hole width (μm)
2:1	352	174
3:1	382	122
4:1	388	98
5:1	400	80
6:1	412	68
12:1	428	35

B. Fabrication of the Grooves on the Gripper Tips

We used a microsecond pulse laser marking machine (HGTECH LU-5 by Huagong Ltd., Wuhan, China) to fabricate grooves on the surface of the 4:1 gripper tip, as shown in Fig. 9(b). The laser spot was positioned at the gripper bottom using a customized motorized positioning platform. The machining was operated with a pulse duration of 1 μs, current of 1 A, scanning speed of 1000 mm/s, frequency of 50 kHz, and processing times of 20 s. Fig. 9(c) shows the groove size by a laser scanning confocal microscopy (Smartproof 5 by ZEISS, Oberkochen, Germany). The groove has a width of 27 μm and a depth of 15 μm.

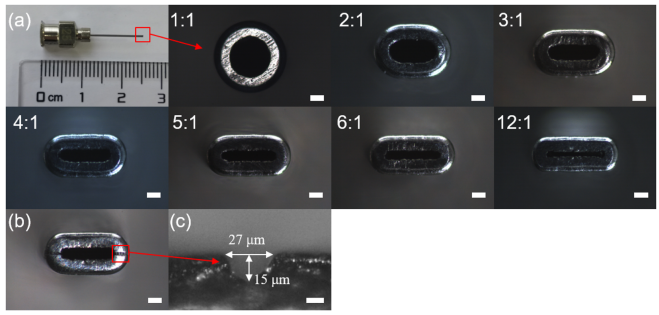

Fig. 9. (a) Commercial 25G stainless needle and the images of the gripper tip with different tip aspect ratios of 1:1, 2:1, 3:1, 4:1, 5:1, 6:1, 12:1. Scale bars: 100 μm. (b) Fabricated gripper tip with micro-grooves. Scale bar: 100 μm. (c) Measurement of micro-groove size. Scale bar: 10 μm.

C. Materials

Glass fiber having a diameter of 13 μm and a length of 4 mm was used in the self-alignment experiments and two-dimensional patterned layout. The carbon fiber (PAN by Toho Tenax Co., Ltd., Japan) with a diameter of 8 μm was used to test the maximum gripping force and glass-capillary insertion experiment. A glass slide sprayed with superhydrophobic nano-coating material (Glaco SOFT99 by Japan Co., Ltd., Japan) is used as the substrate for picking up the microfibers. The superhydrophobic substrate has a static apparent contact angle of 165°. The release substrate is prepared from PDMS (SYLGARD 184 by Dow Corning Co., Ltd., USA), with a proportion of 10:1. The PDMS was spin-coated onto a glass slide substrate (300 r/min, 60 s) and dried at 100 °C for 45 min, resulting in a film thickness of about 100 μm. DI water was used as the liquid in all experiments.

REFERENCES

[1] M. Hejazi, W. Tong, M. R. Ibbotson, S. Prawer, and D. J. Garrett, "Advances in carbon-based microfiber electrodes for neural interfacing," *Front. Neurosci.*, vol. 15, 2021, Art. no. 658703.
[2] J. Andreska, C. Maurer, J. Bohnet, and U. S. Schulz, "Erosion resistance of electroplated nickel coatings on carbon-fibre reinforced plastics," *Wear*, vol. 319, no. 1/2, pp. 138–144, 2014.
[3] W. Lai, L. Cao, J. Liu, S. C. Tjin, and S. J. Phee, "A Three-axial force sensor based on fiber bragg gratings for surgical robots," *IEEE/Amer. Soc. Mech. Eng. Trans. Mechatron.*, vol. 27, no. 2, pp. 777–789, Apr. 2022.
[4] Y. Liu, X. Zhang, Y. Xia, and H. Yang, "Magnetic-field-assisted electrospinning of aligned straight and wavy polymeric nanofibers," *Adv. Mater.*, vol. 22, no. 22, pp. 2454–2457, 2010.
[5] B. G. Compton and J. A. Lewis, "3D-printing of lightweight cellular composites," *Adv. Mater.*, vol. 26, no. 34, pp. 5930–5935, 2014.
[6] J. Daniel et al., "Pearl-chain formation of discontinuous carbon fiber under an electrical field," *J. Manuf. Mater. Process.*, vol. 1, no. 2, pp. 16–18, 2017.
[7] Y. Tian, J. G. Park, Q. Cheng, Z. Liang, C. Zhang, and B. Wang, "The fabrication of single-walled carbon nanotube/polyelectrolyte multilayer composites by layer-by-layer assembly and magnetic field assisted alignment," *Nanotechnology*, vol. 20, no. 33, 2009, Art. no. 335601.

[8] P. R. Patel et al., "High density carbon fiber arrays for chronic electrophysiology, fast scan cyclic voltammetry, and correlative anatomy," *J. Neural Eng.*, vol. 17, no. 5, 2020, Art. no. 056029.
[9] P. Saketi, M. Von Essen, M. Mikczinski, S. Heinemann, S. Fatikow, and P. Kallio, "A flexible microrobotic platform for handling microscale specimens of fibrous materials for microscopic studies," *J. Microsc.*, vol. 248, no. 2, pp. 163–171, 2012.
[10] W. F. Gillis et al., "Carbon fiber on polyimide ultra-microelectrodes," *J. Neural Eng.*, vol. 15, no. 1, 2018, Art. no. 016010.
[11] H. N. Schwerdt et al., "Subcellular probes for neurochemical recording from multiple brain sites," *Lab Chip*, vol. 17, no. 6, pp. 1104–1115, 2017.
[12] G. Arutinov et al., "Capillary gripping and self-alignment: A route toward autonomous heterogeneous assembly," *IEEE Trans. Robot.*, vol. 31, no. 4, pp. 1033–1043, Aug. 2015.
[13] A. Iazzolino, Y. Tourtit, A. Chafaï, T. Gilet, P. Lambert, and L. Tadrist, "Pick up and release of micro-objects: A motion-free method to change the conformity of a capillary contact," *Soft Matter*, vol. 16, no. 3, pp. 754–763, 2020.
[14] W. Hagiwara, T. Ito, K. Tanaka, R. Tokui, and O. Fuchiwaki, "Capillary force gripper for complex-shaped micro-objects with fast droplet forming by on-off control of a piston slider," *IEEE Robot. Automat. Lett.*, vol. 4, no. 4, pp. 3695–3702, Oct. 2019.
[15] B. Chang, Y. Feng, J. Jin, and Q. Zhou, "Low-cost laser micromachining super hydrophilic–super hydrophobic microgrooves for robotic capillary micromanipulation of microfibers," *Micromachines*, vol. 12, no. 8, 2021, Art. no. 854.
[16] B. Chang, B. K. Wang, J. L. Jin, and Q. Zhou, "Capillary pick-and-place of glass microfibers," *IEEE Access*, vol. 9, pp. 15074–15083, 2021.
[17] V. Sariola, V. Liimatainen, T. Tolonen, R. Udd, and Q. Zhou, "Silicon capillary gripper with self-alignment capability," in *Proc. IEEE Int. Conf. Robot. Automat.*, 2011, pp. 4098–4103.
[18] B. Chang, Y. H. Feng, J. L. Jin, and Q. Zhou, "Ejected droplet-directed transportation and self-alignment of microfibers to micro trenches," *J. Microelectromech. Syst.*, vol. 30, no. 5, pp. 751–758, Oct. 2021.
[19] M. Mastrangeli, Q. Zhou, V. Sariola, and P. Lambert, "Surface tension-driven self-alignment," *Soft Matter*, vol. 13, no. 2, pp. 304–327, 2017.
[20] B. Chang, Z. Zhu, M. Koverola, and Q. Zhou, "Laser-assisted mist capillary self-alignment," *Micromachines*, vol. 8, no. 12, 2017, Art. no. 361.
[21] H. Matsui, Y. Noda, and T. Hasegawa, "Hybrid energy-minimization simulation of equilibrium droplet shapes on hydrophilic/hydrophobic patterned surfaces," *Langmuir*, vol. 28, no. 44, pp. 15450–15453, 2012.
[22] K. A. Brakke, "The surface evolver," *Exp. Math.*, vol. 1, no. 2, pp. 141–165, 1992.
[23] L. Song, "GitHub repository," 2023. [Online]. Available: https://github.com/LonggangSong/Supplementary-Code-Surface-Evolver.git
[24] J. N. Israelachvili, "Van der Waals Forces between particles and surfaces," *Intermolecular Surf. Forces*, pp. 253–289, 2011.
[25] M. J. Hokkanen, M. Backholm, M. Vuckovac, Q. Zhou, and R. H. A. Ras, "Force-based wetting characterization of stochastic superhydrophobic coatings at nanonewton sensitivity," *Adv. Mater.*, vol. 33, no. 42, 2021, Art. no. 210513.

Longgang Song received the B.Sc. degree in mechanical design manufacturing and automation technology from Xi'an Polytechnic University, Xi'an, China, in 2016. He is currently working toward the Ph.D. degree in light industry equipment and control with the Shaanxi University of Science and Technology of Mechatronics Engineering, Xi'an, China.

His research interests include robotic microassembly, capillary gripper, and wettability detection.

Bo Chang received the M.Sc. degree in automation technology from the Tampere University of Technology, Tampere, Finland, and the Dr. Tech. degree in electrical engineering from Aalto University, Espoo, Finland, in 2003 and 2013, respectively.

From 2013 to 2016, she was an Academy Postdoctoral Researcher with the Robotic Instruments Laboratory, Aalto University. Since 2017, she has been a Professor with the School of Mechatronics Engineering, Shaanxi University of Science and Technology, Xi'an, China. Her research interests include robotic microassembly, self-assembly, micromanipulation, microrobotics, and applications.

Yuhang Feng received the B.Sc. degree in mechanical design manufacturing and automation technology in 2019 from Shaanxi University of Science and Technology, Xi'an, China, where he is currently working toward the M.Sc. degree in mechanical engineering with the School of Mechatronics Engineering.

His research interests include laser microfabrication and microassembly.

Jialong Jin received the B.Sc. degree in mechanical design manufacturing and automation technology in 2018 from the Shaanxi University of Science and Technology, Xi'an, China, where he is currently working toward the master's degree in mechanical engineering with the School of Mechatronics Engineering.

His research interests include capillary self-alignment and robotic assembly.

Quan Zhou (Member, IEEE) received the M.Sc. degree in control engineering and the Dr. Tech. degree in automation technology from Tampere University of Technology, Tampere, Finland, in 1996 and 2004, respectively.

He is currently a Full Professor leading the Robotic Instrument Group with the Department of Electrical Engineering and Automation, School of Electrical Engineering, Aalto University, Espoo, Finland. His main research interests include miniaturized robotic instruments, micromanipulation, and related automation methods.

Dr. Zhou is currently a Coordinator of the Miniaturized Robotics Topic Group of the European Robotics Association (euRobotics). He was also a Coordinator of EU FP7 Project FAB2ASM, the first PPP Project of the European Economic Recovery Plan. He was the General Chair of International Conference on Manipulation, Automation and Robotics at Small Scales, MARSS 2019. He was also the Chair of IEEE Finland Joint Chapter of Control System Society, Robotics and Automation Society, and System Man and Cybernetics Society.